Femtosecond time-resolved spectroscopic studies of the dynamics of the relaxation of excitons in the lowest adiabatic potential energy surface in NaCl

1994 J. Phys.: Condens. Matter 6 4581

(http://iopscience.iop.org/0953-8984/6/24/018)

J. Phys.: Condens. Matter 6 (1994) 4581–4600. Printed in the UK

Femtosecond time-resolved spectroscopic studies of the dynamics of the relaxation of excitons in the lowest adiabatic potential energy surface in NaCl

T Makimura†, K Tanimura†, N Itoh†, T Tokizaki‡ and A Nakamura‡

† Department of Physics, Faculty of Science, Nagoya University, Furo-cho, Chikusa 464-01, Japan

‡ Department of Applied Physics, Faculty of Engineering, Nagoya University, Furo-cho, Chikusa 464-01, Japan

Received 5 January 1994, in final form 1 March 1994

Abstract. We have measured time-resolved optical absorption spectra following the excitation of the self-trapped excitons (STEs) in NaCl from the lowest triplet state to the next higher electron-excited state. In addition to the rapid reduction of the band due to the electron transition of the STE (STE band), a new absorption band peaked between the STE band and the F band is found to be temporarily generated. The heights of the new band and that of the STE band show anticorrelated oscillations with a period of 1 ps and moreover the new band disappears and the STE band recovers within 7 ps after the excitation. It is shown that the new band is due to the transition from the adiabatic potential energy surface on which the lowest STE is located and the oscillation is interpreted to be a motion of a wave packet on the adiabatic potential energy surface. We find also that the F band grows in the relaxation process.

1. Introduction

The phenomena associated with strong local lattice rearrangement induced by excitation of either bulk or defect electronic states are observed in many non-metallic solids [1, 2]. These include exciton self-trapping [3, 4], intrinsic lattice defect production [5, 6], atomic desorption from the surface [7], defect migration and reactions upon electron–hole recombination [2], metastability and bistability of several deep-level defects in compound semiconductors [2], and structural change in amorphous [8] and low-dimensional materials [9, 10]. In order to understand the microscopic processes of these phenomena, which arise from strong coupling of the electronic system with particular modes of the lattice vibration, it is important to trace the dynamics of the relaxation following electronic excitation on the time scale of lattice vibrations.

The self-trapping of excitons and the formation of vacancy (F centre)–interstitial (H centre) pairs in alkali halides are the best studied examples of local lattice rearrangement induced by bulk electronic excitation. The self-trapped excitons (STEs), which are generated either by the relaxation of an exciton [11] or by trapping of an electron by a self-trapped hole or an X_2^- (X is a halogen atom) molecular ion in a D_{2h} symmetry [12–14], exhibit characteristic luminescence (the STE luminescence). The luminescence features a large Stokes shift, the amount of which depends not only on the spin multiplicity (singlet or triplet) of the initial state of the luminescence, but also on the kind of alkali halide. The STE luminescence bands in nine alkali halide crystals, consisting of three alkalis Na, K,

0953-8984/94/244581+20$19.50

Rb and of three halogens Cl, Br, I have been classified into three types by Kan'no *et al* [15] based on the relation between the Stokes shift normalized by the energy of the lowest exciton absorption peak and the Rabin–Klick parameter S/D [16], where S is the space between two adjacent halogen ions and D is the diameter of the halogen atom. The three types are named type I, type II and type III in ascending order of Stokes shift, namely the lattice relaxation energy of the luminescent state increases in this order. The STEs exhibit not only the luminescence, but also the optical absorption bands due to transitions of their electron and hole components. Tanimura and Itoh have shown that the STEs can be grouped also in terms of the Mollwo–Ivey relation (the plot between the absorption peak energy and the lattice constant) for the lowest electron transition energy [17], yielding almost exactly the same classification as made in terms of the Stokes shift. Thus the classification into three types is related directly to the difference in the configuration of the STEs. Hereafter we use the notations type I STE, type II STE and type III STE to distinguish the relaxed configurations.

Only one type of STE is formed in some alkali halides, whereas two types of STE are formed in many alkali halides and all three types are formed in RbI [18]. The existence of several configurations of STEs for a given alkali halide reflects the structure of the adiabatic potential energy surface (APES) for the lowest state of the exciton, on which theoretical studies have been carried out by several authors. Toyozawa has argued that the STE having a D_{2h} configuration (the on-centre configuration), a hole relaxed into a V_K centre with a bound electron, has an adiabatic instability [19]. Leung and co-workers extended this concept and showed that the APES has a minimum at a configuration where the X_2^- molecular ion is displaced by an X–X distance in the lattice, forming the nearest pair of an F centre and an H centre [20, 21]. Recent studies of the lowest APES with respect to the displacement and rotation of the X_2^- molecular ion strongly suggest that the APES has multiple minima near the close F–H pair configurations and that the APES near the minima is extremely flat with low characteristic frequencies [22].

Because of the presence of the optical absorption band in the infra-red [23] and its smallest Stokes shift [15], the type I STE has been proposed to have the on-centre configuration [15, 24]. Recent study of the resonance Raman scattering of the triplet STEs in NaBr [25], which has been assigned to a type I STE, has provided direct evidence for this interpretation. The large Stokes shifts for the luminescence bands of type II and III STEs and the peak energies of the optical absorption band near the corresponding F-band peaks suggest that these STEs are close to the nearest F–H pairs, evidenced further by the recent resonance Raman scattering spectroscopy [25]. The fact that luminescence bands of both type II and type III are observed in RbI indicates that the lowest triplet APES in RbI has two minima corresponding to these two types of STE. The singlet luminescence (the σ luminescence) in alkali halides is of type I, indicating that the singlet state of the STE can luminesce from the on-centre configuration. On the other hand, the triplet STE luminescence (the π luminescence) in alkali halides except NaBr and NaI is assigned either to type II or type III, indicating that the triplet STEs involve the off-centre displacements. In NaCl, which is used in the present investigation, the singlet luminescence is ascribed to the emission from the type I STE. However, classification of the triplet STE in NaCl is somewhat ambiguous; it exhibits the optical absorption band assigned to type II [17], but the Stokes shift of the π luminescence lies between those for type II and type III for the corresponding value of S/D [15].

Creation of electron–hole pairs is known to lead to formation of F–H pairs as well as the STEs. Tanimura has shown that the sum of the yields of the triplet STEs and of the F–H pairs generated by an single 1 MeV electron pulse at 5 K does not depend on the alkali halide,

although each yield depends strongly on the kind of alkali halide [26]. Furthermore the temperature dependence of the F centre yield in KI, RbI, NaBr, NaCl and LiCl was found to be anticorrelated to the triplet STE (π) luminescence intensity [27]. It has been observed also that excitation of the triplet STEs produces the F centres [28–30]. These observations indicate clearly that the F–H pair is one of the major products generated by relaxation of electron–hole pairs. The mechanism leading to the F–H pair configuration from the STE configuration has been studied by many authors [6, 19, 31–35]. It is now generally accepted that two types of F–H pair generation process exist: one is the thermally activated process by which the lowest-STE configuration is transferred into the F–H pair configuration on the lowest APES, and the other is a dynamical process in which F–H pairs are generated from an excited (electronically and/or vibrationally) state of the STE during its relaxation. Although the former process has been evidenced experimentally by means of time-resolved spectroscopy in the picosecond time regime [36, 37], the mechanism of the latter process is still controversial as reviewed recently [5].

The de-excitation process of electron–hole pairs to the lowest APES of excitons in alkali halides includes several sequential steps: cooling of electrons and holes in the conduction and valence bands, respectively, trapping of an electron by a self-trapped hole leading to formation of highly excited states of the STE, successive de-excitation through excited states including non-radiative transitions and lattice relaxation. The dynamics of the STE and F–H pair formation processes have been studied by time-resolved optical measurements. The formation time of the F centres was first observed on the time scale of picoseconds by Bradford *et al* in 1975, using 20 ps laser pulses for electron–hole pair generation and 30 ps laser pulses for detection [38]. They showed that the ground states of the F centres in KCl are created within 10 ps after electron–hole pair generation. Williams *et al*, using a convolution technique, determined the formation time of the F centres in KCl to be 9 ± 5 ps and the lowest triplet state of STEs in NaCl to be much shorter [39]. Time-resolved absorption spectra after electron–hole pair generation in NaCl have been measured using picosecond white light pulses as the probe [36]. It has been shown that a broad absorption band appears at an energy range between the STE and F-band maxima as a primary product. Although it has been found that the broad band is converted to the STE band at 80 K and to the F band at 300 K at several hundred picoseconds after excitation, neither the origin of the primary absorption band nor its relaxation pathways to the F–H pair has been clarified.

Williams *et al* suggested that the F–H pairs separated by more than two X–X distances are generated as a result of the dynamic lattice relaxation on the lowest APES after the electronic transition from the next higher state [6]. The idea is primarily based on the off-centre instability of the on-centre STE; the excess energy at the on-centre STE with respect to the off-centre STE is transferred to the kinetic energy for the dynamical motion of the X_2^- molecular ion to the further distant F–H pair configuration. No experimental evidence has been obtained for this dynamic relaxation on the lowest APES of the exciton. As described above, the lowest APES of the exciton in alkali halides has the interesting feature of a possible multiple-minima structure with low characteristic frequencies. The dynamics of the relaxation on such an APES is not only of interest for elucidating the mechanism of defect formation in alkali halides, but is also useful for understanding similar processes induced by electronic excitation both in the bulk and on the surfaces of several systems. In order to reveal the dynamics of relaxation on the lowest APES, we need to use laser pulses with a duration shorter than the period of the lattice vibration associated with the lowest APES and to follow the de-excitation not from the electron–hole pairs but from the low-lying excited states.

Using short-pulse techniques, we have investigated the relaxation of the STEs in NaCl

after excitation from the lowest triplet STEs to the electron excited state in a time scale of 100 fs. Hereafter we use the term STE to indicate the lowest triplet STE unless otherwise remarked. The STEs are populated by a KrCl laser pulse and are excited further with a subsequent femtosecond laser pulse. The changes in optical absorption spectra due to relaxation of the excited state are probed by a femtosecond white light pulse. We find the generation of a new band accompanied by the reduction of the band due to STEs, referred to as the STE band hereafter. Oscillations with a period of 1 ps are observed in the height of the STE band and that of the new band: the time correlation is such that the minimum of the former and the maximum of the latter occurs at the same time. The height of the STE band recovers to reach a constant value (90% of the initial optical absorption strength) within 7 ps and the new band disappears at the same time. We also find that the F band is created during the relaxation process. A brief description of these results has been given elsewhere [40]. In this paper, we present a full description of the results and their detailed analysis, and discuss the de-excitation processes from the excited state of the STE: the non-radiative electronic transition to the lowest STE, the dynamic relaxation on the lowest APES and the resulting dynamic F-centre formation.

2. Experimental details

The samples used in the present work were cleaved to a size of $10 \times 10 \times 5$ mm^3 from a block of NaCl crystal purchased from Harshow Chemical Co. A specimen was mounted in a cold finger of a cryostat and was cooled through a thermal contact to a liquid helium reservoir. A schematic diagram of the experimental apparatus for the time-resolved optical absorption measurements is shown in figure 1. In order to populate the sample with the STEs, laser pulses of 222 nm in wavelength and 15 mJ in fluence generated by a KrCl excimer laser (Lambda Physik, EMG201MSC) were incident on the specimen. The STEs thus generated were excited further with subsequent 605 nm laser pulses and the time-resolved optical absorption spectra were measured using a femtosecond spectroscopic system. A pulse generator triggered both the excimer laser pulse and the 605 nm femtosecond pulse so that the latter was delayed by 5 μs from the former.

The 605 nm pulses were generated by a synchronously pumped, cavity-dumped dye laser (Spectra-Physics, Model 375B) with Rhodamin 6G and saturable dye DQOCI. The dye laser was pumped by a mode-locked Ar^+ laser (Spectra-Physics, Model 2030). The dye laser pulses were compressed by a grating–prism pair to a duration of 80 fs. Then they were amplified by a three-stage dye amplifier with Kitonred, pumped by an XeCl excimer laser (Lambda Physik, EMG 103MSC) or a YAG laser (Continuum, Model 661-10). After amplification, they were compressed again by a pair of prisms. The output pulses from this system had an energy of 50 μJ. From the auto-correlation traces of these pulses, the pulse width was determined to be 130 fs by assuming a hyperbolic-secant-squared pulse shape. The femtosecond laser pulse beam F_1 was split into two parts by a half mirror HM_1. One of them P_2 was used for the excitation of the STEs at the lowest triplet state. The other beam F_2 was focused on a D_2O cell to generate white light pulses ranging from 400 nm to 700 nm. The beam W of white light was split further by a half mirror HM_2 into the reference beam W_0 and the probe beam W_1, the latter of which was focused onto the sample S. The travelling distances of the probe beam and of the excitation beam were adjusted by a delay line D. Because of the group velocity dispersion in lenses, the delay time $\tau(\lambda)$ of the white light pulse for probing with respect to the excitation pulse depends on the wavelength. $\tau(\lambda)$ was determined by measuring cross correlation signals between the probing and excitation pulses using a KDP crystal placed on the sample position.

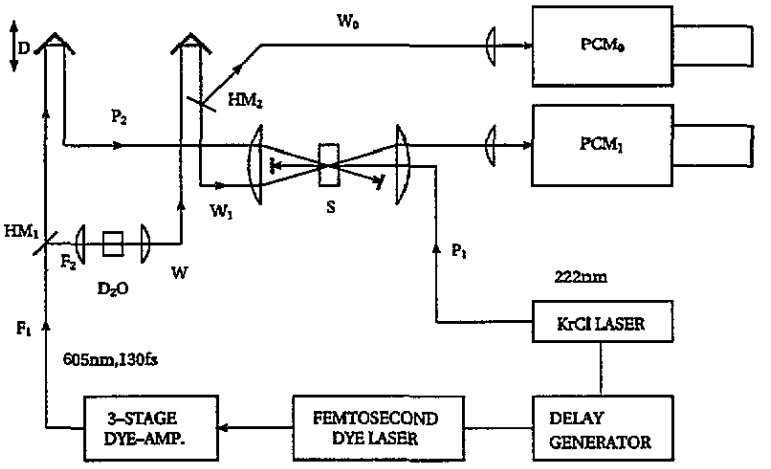

Figure 1. A schematic diagram of the experimental set-up for measurements of time-resolved optical absorption spectra on a femtosecond time scale. A 222 nm KrCl pulsed laser beam P_1 with a pulse duration of 20 ns populated an NaCl specimen S kept at liquid helium temperature with the self-trapped excitons in the lowest triplet state by two-photon absorption. A femtosecond pulsed laser beam F_1 synchronized to the KrCl laser pulse was divided into two beams F_2 and P_2 with a half mirror HM_1. The white light pulsed beam W for probing is generated by passing F_2 through a D_2O cell. The delay of W relative to P_2 is adjusted using the delay line D. W is divided further into two beams W_1 and W_0 with a half mirror HM_2. The beams W_1 after passing through S and the beam W_0 are led to polychromators PCM_1, PCM_0 respectively.

The reference beam W_0 and the probe beam W_1 through the sample were led to polychromators, PCM_0 and PCM_1, consisting of grating monochromators (Jobin Yvon, HR320) and photodiode array detectors (Princeton RY1024). The output signals of the arrays for reference and probing beams were processed by a controller (Princeton Instruments, ST-110P) and stored in a personal computer. The transmittance as a function of delay time was calculated using the ratio of the intensities of the probe and reference pulses.

3. Results

The femtosecond time-resolved spectra were measured after excitation with 605 nm laser pulses from the lowest 1s-like state to the 2p-like state of the STE in NaCl at 5 K. Figure 2(a) shows the optical absorption spectrum probed before 605 nm excitation; the optical absorption simply represents the band due to the electron transition of the lowest STEs, or the STE band. To show the changes in optical absorption spectra caused by the excitation of the STEs clearly, we subtracted the spectrum of figure 2(a) from the optical absorption spectra at several delay times (τ_d) after the excitation. The results thus obtained are shown in figure 2(b). Obviously, the height of the STE band is reduced at a τ_d of 0.2 ps. Besides the reduction in the height of the STE band, an increase of the optical absorption is induced in the range from 2.1 eV to 2.5 eV in photon energy at a τ_d of 1.0 ps. We call this band the X band. At a τ_d of 8 ps, the height of the STE band almost recovers and the height of the X band is reduced.

In order to decompose each curve shown in figure 2(b) into the STE and X bands, we analysed each curve in figure 2(b) in the following way. Referring to figure 3, in which

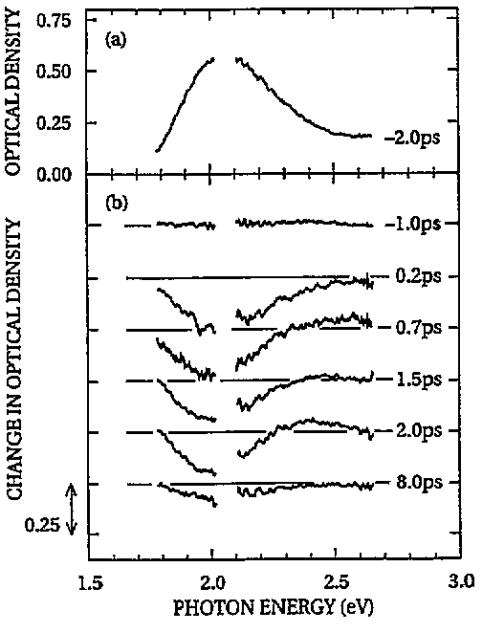

Figure 2. The transient optical absorption spectrum due to the self-trapped exciton in NaCl produced with a 222 nm KrCl laser pulse at liquid helium temperature (a) and the changes in the time-resolved optical absorption spectra at various delay times after successive excitation of the generated self-trapped excitons with a 130 fs laser pulse of 605 nm (b). The STE spectrum was obtained with a negative delay time of −2.0 ps.

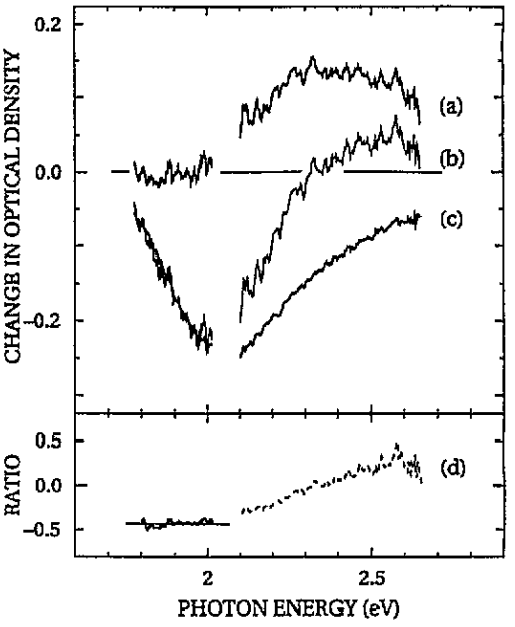

Figure 3. The result of the analysis of the optical absorption change at a time delay of 0.7 ps induced by 605 nm excitation of the self-trapped excitons. A replot (b) of the result shown in figure 2(b) is divided into the decrement of the STE band (c) and the increasing component (a). Curve d is the photon energy dependence of the ratio of curve b to the STE band produced by a 222 nm laser pulse.

curve b represents the absorption spectrum at a τ_d of 0.7 ps in figure 2(b), we first calculated the ratio of the magnitudes of curve b to those of the optical absorption curve shown in figure 2(a) at each photon energy. As shown in figure 3(d), the ratio is evidently constant in the range of 1.8–2.0 eV. The constant ratio is represented as $R(\tau_d) - 1$, where the ratio $R(\tau_d)$ corresponds to the fraction of the STEs present at τ_d after the excitation. Using this ratio, we determined the reduction of the STE band as shown by curve c. The difference between curves b and c gives the optical absorption spectrum generated by the excitation of the STE. Apparently, 1s–2p excitation of the STEs reduces their concentration and transfers them partially to the new centres giving rise to the X band.

Spectra of the induced absorption at several τ_d values are shown in figure 4. A single absorption band is discernable at a τ_d of 0.9 ps, while two absorption bands can be seen at a τ_d of 3 ps. The peak of the band that appears at a τ_d of 0.3 ps shifts to the low-energy side and its width becomes narrower, while the other band has a peak at 2.75 eV irrespective of τ_d. The latter band is identified as the F band in NaCl. The half width and the peak energy of the X band are shown as functions of τ_d in figure 5(a) and (b), respectively. Although the F band and X band can be clearly resolved for $\tau_d > 3.0$ ps as seen in figure 4, the resolution is not evident for smaller τ_d. In this time range, we evaluated the upper bound of the half width by assuming that the whole band is the X band and the lower bound by assuming that the spectrum is a composite of the F and X bands. The upper and lower bounds are indicated by the error bars in figure 5. Similar consideration is made in the error bars for the peak energy. From this result, the band width of the X band is 0.6 eV

immediately after the excitation and decreases gradually to a constant value 0.2 eV at a τ_d of 7 ps. The peak energy of the X band shifts from 2.5 eV to 2.25 eV.

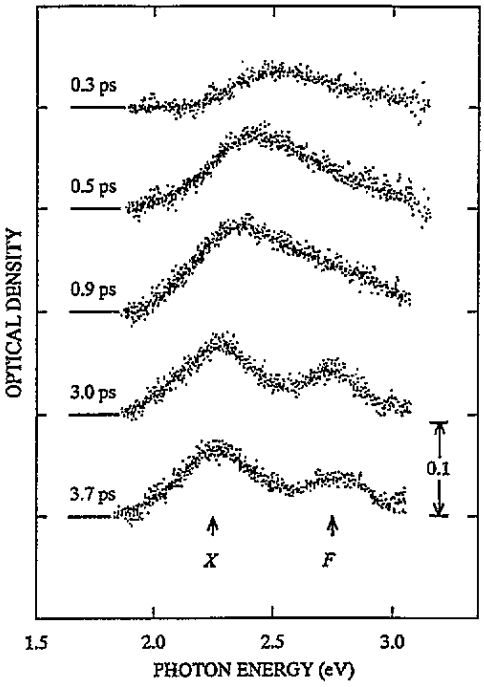

Figure 4. The increment of optical absorption spectra induced by excitation with a 605 nm laser pulse of the self-trapped excitons in NaCl, obtained with the method shown in figure 3(a).

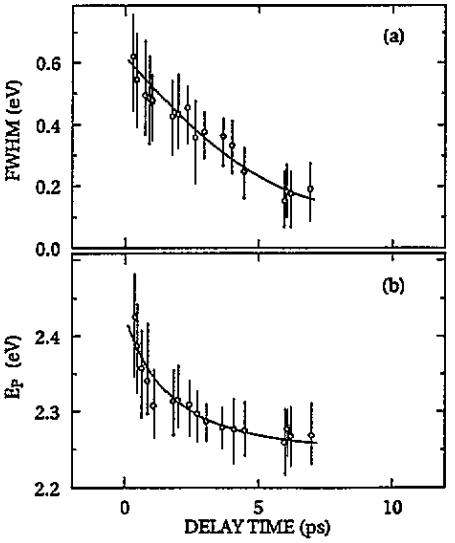

Figure 5. (a) The width (FWHM) and (b) the peak position (E_p) of the X band plotted as a function of delay time after excitation with a 605 nm laser pulse.

The fraction $R(\tau_d)$ of the STE at τ_d, as defined before, is shown by open circles in figure 6(a). $R(\tau_d)$ first decreases from 1.0 to 0.56 within the pulse duration. Then it shows a rapid partial recovery followed by a decrease to reach a minimum at a τ_d of 1 ps, and then increases gradually showing an oscillatory behaviour with a period of 1.0 ps. It reaches a constant value within 7 ps. About 10% of the STEs present before the excitation are eliminated finally by laser irradiation. In order to investigate the temporal change of the X band, we plot in figure 6(b) the optical density $X(\tau_d)$ at 2.35 eV as a function of τ_d. $X(\tau_d)$ grows first, reaching a maximum at τ_d of 1 ps, and then decays within 7 ps showing an oscillation with a period of 1 ps. It is clear that $R(\tau_d)$ and $X(\tau_d)$ are closely correlated: the periods of the oscillations of $R(\tau_d)$ and $X(\tau_d)$ are the same and their oscillations are opposite in phase. Furthermore the overall recovery of $R(\tau_d)$ is anti-correlated to the overall decay of $X(\tau_d)$.

In order to evaluate the temporal change of the height $F(\tau_d)$ of the F band, we decomposed each of the optical absorption curves shown in figure 4 into two Gaussians, one due to the X band and the other due to the F band. $F(\tau_d)$ as a function of τ_d is plotted in figure 6(c). We note that the initial growths of $X(\tau_d)$ and $F(\tau_d)$ for $\tau_d < 1$ ps are almost in parallel and both $X(\tau_d)$ and $F(\tau_d)$ show an overall increase until 2 ps and then decrease gradually.

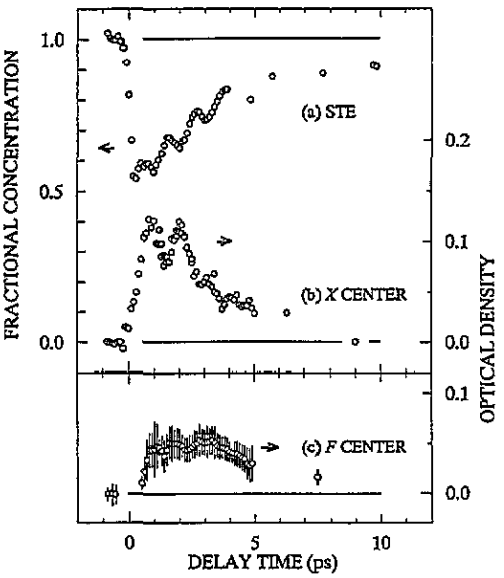

Figure 6. (a) Fractional change of the STE concentration after excitation with a 605 nm laser pulse and the resulting change in the X-band height (b) and F-band height (c). The changes in the X-band heights are derived by analysing the results as shown in figure 4.

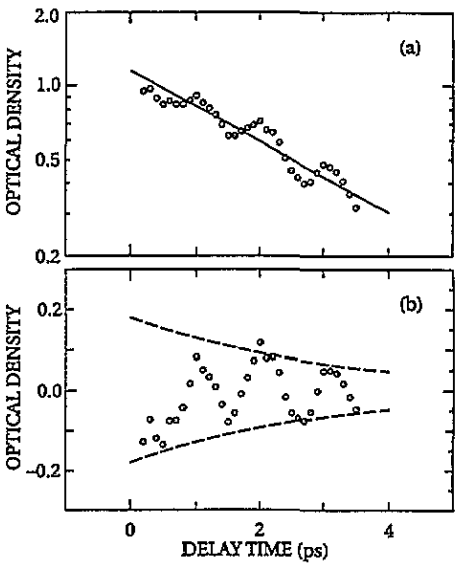

Figure 7. (a) A semilogarithmic plot of the recovery of the self-trapped excitons reduced by excitation with a 605 nm laser pulse; the solid line indicates the overall recovery. The difference between the experimental results (circles) and the solid line is shown in (b); the dashed lines show the envelope of the oscillation.

4. Discussion

4.1. Major features of the relaxation process from the 2p-excited STE

From the results of the recovery of the STE band and the decay of the X band, it is evident that the centre (X centre) which gives rise to the X band is an intermediate formed in the process of recovery after excitation to the 2p-excited STE, which is an electron excited at the 2p-like state. The primary question now arises of whether the X centre represents a state on the lowest or excited APES. In figure 3, we have resolved the X band generated and the STE band bleached. It is seen that the integrated area of the X band generated is about 0.5 times that of the STE band bleached. Since the X centre is formed by exciting the lowest STE, its concentration cannot be larger than that of the lowest STEs bleached. It follows that the oscillator strength of the X band transition is of the same order of magnitude as the 1s–2p electron transition of the STE, which is known to be close to unity [41].

The high oscillator strength for the transition from the X centre suggests that it is on the lowest APES. Suppose that the X centre represents a state on the 2p-excited APES. Then any transition of this energy range reaches the conduction band and, in such a case, the oscillator strength is much smaller than unity, as is well known for the L band due to the electron transition to the continuum of the F centre [42], for which the oscillator strength is smaller by a factor of 100 than that of the F band, which corresponds to the 1s–2p transition. Furthermore, the temporally anti-correlated oscillation between the X and STE band heights for a few picoseconds after the excitation can be accounted for only by a transfer between the two states on the same APES. From these considerations, we conclude that the X centre and the STE represent local minima on the lowest APES.

We emphasize three major experimental features of the temporal change of the STE, X and F bands. The most striking feature is the anti-correlated oscillation: when the STE band height takes a minimum, the X-band height takes a maximum. As we discussed above, the oscillation represents the mutual transfer between the X-centre configuration and the STE configuration on the lowest APES. This transfer reflects the dynamics of the relaxation on the lowest APES. The second feature is concerned with the difference in the temporal changes of the STE band and X band seen in the early stage of relaxation. The STE band bleached by the excitation recovers partially within 1 ps and then decreases again leading to a minimum at 1 ps. On the other hand the X band continues to grow and reaches a maximum at 1 ps; there is no minimum in the X-band growth corresponding to the first maximum of the temporal change in the STE-band height. The absence of this minimum is considered to be related to the relaxation route on the lowest APES after non-radiative transition from the 2p-excited STE and suggests strongly that the non-radiative transition from the 2p-excited state does not lead directly to the X-centre configuration but to the STE configuration. The third feature is seen in the growth of the F band. As seen in figure 6, the growth of the F band takes place almost parallel to the growth of the X band; the rise time of the F band is not less than that of the X band.

In order to find a key factor which governs the features mentioned above, we pay attention to the recovery of the STE absorption band as a function of τ_d. We replot the bleached height of the STE band minus the permanently bleached fraction of about 10% of the initial height of the STE band as a function of τ_d on a semilogarithmic scale in figure 7(a). The temporal change in $R(\tau_d)$ can be interpreted as a superposition of two components; the exponentially decaying component with a time constant τ_L of 3 ps shown by the solid line and the oscillatory component. The latter is obtained by taking the difference between the experimental data and the solid line and is shown in figure 7(b). It is seen that the amplitude of the oscillatory component decreases with increasing time; the decrease is characterized by a time constant τ_P of ~ 3 ps as shown by dashed curves, which shows the envelope of the oscillation. The factorization of the recovery curve can be understood in terms of the wave packet dynamics; the time constant τ_L corresponds to the energy relaxation rate, while the time constant τ_P corresponds to the phase relaxation rate. We presume that the relaxation process on the lowest APES is governed by the dynamics of a wave packet generated upon the non-radiative transition from the 2p-excited STE.

In order to obtain a deeper understanding of the relaxation process of the STE in NaCl, we first propose a model which can explain all of these features, and then we analyse the experimental results quantitatively to examine the validity of the model.

4.2. The model of the relaxation of the 2p-excited STE in NaCl

The essential points of our model are shown schematically in figure 8. Based on the conclusion that the STE and the X centre represent two configurations on the lowest APES, we introduce the lowest APES with two minima, corresponding to the STE and the X centre. Upon excitation of the lowest STE, which is the STE in the electronically and vibrationally lowest state, to the 2p-excited state, non-radiative transition to the lowest APES takes place. We presume that the state regenerated initially by this non-radiative transition is not the X centre but the STE at the minimum electronically but excited vibrationally. The 'hot' STEs thus restored to the lowest APES are finally thermalized into the lowest STE, but the thermalization includes a dynamical relaxation process which can be described as a motion of a wave packet coherently propagating on the APES with double minima at a natural oscillation frequency. During this dynamical process, transfer between the STE configuration and the X-centre configuration takes place until the coherence of the packet is lost and the

excess vibrational energy is dissipated. The F centres are formed with a certain probability during the wave packet motion, and this conversion into the F–H pair configuration causes a loss of the initial concentration of the lowest STE. This is the whole story of the de-excitation process after formation of the 2p-excited STE in NaCl. In the following sections, we analyse the experimental results quantitatively to examine the validity of our model.

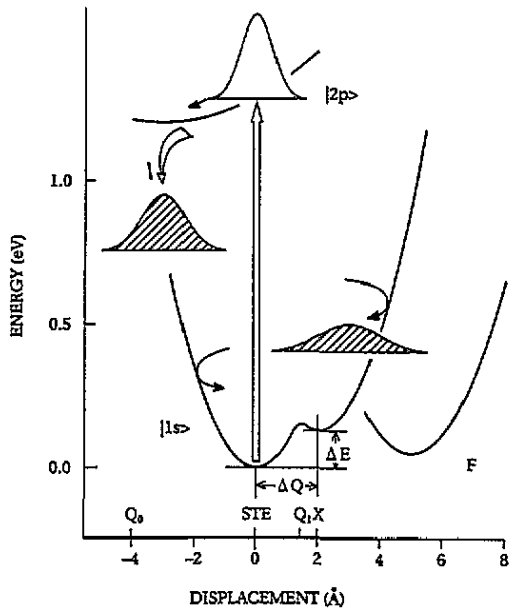

Figure 8. The adiabatic potential energy surface of the lowest state of the STE used for the simulation of the dynamics of relaxation. The STE configuration is taken as 0 displacement and X corresponds to the X-centre configuration. Q_0 is the position where the packet is placed on the lowest APES and Q_1 indicates the crossing of the two parabolas for the lowest excited state. The curve F denotes schematically the adiabatic potential energy surface having a minimum at the F-centre configuration.

4.3. Analysis of the experimental results

In order to analyse experimental results quantitatively, we need to simulate the de-excitation processes after excitation to the 2p-excited STE. In view of the model shown in figure 8, the following two factors are crucial: the time-dependent rate of repopulation onto the lowest APES and the motion and thermalization on the lowest APES of the packet formed by the repopulation. The former factor may be governed by several steps including the de-excitation within the APES for the 2p-excited STE and the non-radiative transition to the lowest APES. The sequence of these steps will produce a time delay for the repopulation and an additional distribution with respect to time on the rate of repopulation on the lowest APES or on the rate of generation of packets. In order to evaluate the rate of repopulation from the experimental results, we analysed the temporal change of the STE- and X-band heights at the very beginning after excitation, namely for $\tau_d = 0$–1 ps, using rate equations. This treatment is phenomenological, but is of use to derive the initial conditions for the motion of the wave packet from the experimental data. Using the parameters derived from this analysis, we simulate the dynamical relaxation of the lowest APES.

4.3.1. The time dependence of the repopulation onto the lowest APES. A characteristic feature of curve a in figure 6 is a rapid partial recovery of bleaching of the STE band; after the decrease in optical density due to depopulation by photoexcitation, it recovers, although only partially, and then decreases again within 1 ps [43]. We analyse the results in this time regime in terms of rate equations to describe satisfactorily this rapid partial recovery of the STE band. We use the level diagram shown in the inset of figure 9, where the lowest STE, the 2p-excited STE, the X centre and the 'hot' STE are included. We assume that the hot STE contributes to the optical absorption similarly to the lowest STE but the transformation into the X centre can occur only from this hot state. The occupation numbers of the lowest STE, the 2p-excited STE, the X centre and the hot STE are designated as n_S, n_p, n_X and n_H, respectively. These quantities are governed by the rate equations

$$\frac{dn_S}{dt} = -\sigma\,\phi(t)n_S \tag{1a}$$

$$\frac{dn_p}{dt} = \sigma\,\phi(t)(n_S + n_H) - k_1\,n_p \tag{1b}$$

$$\frac{dn_H}{dt} = -\sigma\,\phi(t)\,n_H + k_1\,n_p - k_2\,n_H \tag{1c}$$

$$\frac{dn_X}{dt} = k_2\,n_H - k_3\,n_X \tag{1d}$$

where $\phi(t)$ is the flux representing the pulse shape of the excitation light, σ is the cross-section of the optical transition, and k_1, k_2, k_3 stand for the non-radiative transition rate from the 2p-excited STE to the hot STE, the rate of transformation from the hot STE to the X centre, and the decay rate of the X centre, respectively. Since the femtosecond light pulse to excite the STE has a finite pulse width of 130 fs, a pulse shape function should be treated explicitly in solving the rate equations. We assumed

$$\phi(t) \propto \operatorname{sech}^2 \frac{t}{T} \tag{2}$$

where $T = 0.074$ ps. Then the rate equations are solved numerically under the following initial conditions:

$$n_S(-\infty) = 1 \tag{3a}$$

$$n_p = n_H = n_X = 0 \qquad \text{at } t = -\infty. \tag{3b}$$

In order to correlate the calculated results with the experimental results, the results of the calculation have to be convoluted with respect to the pulse shape $\phi_p(t)$ of the probe light with finite width. We assumed that ϕ_p is the same in shape as the exciting light pulse. Thus, the convoluted occupation number N_j ($j = X, S, H, p$) of each state, which can be compared directly to the experimental results, is given by [44]

$$N_j(\tau_d) = \int \phi_p(t) n_j(\tau_d + t)\,dt. \tag{4}$$

We obtained the best fit of $N_H(\tau_d) + N_S(\tau_d)$ with the experimental results $R(\tau_d)$ of the temporal change of the STE concentration and of $N_X(\tau_d)$ with the similar temporal change

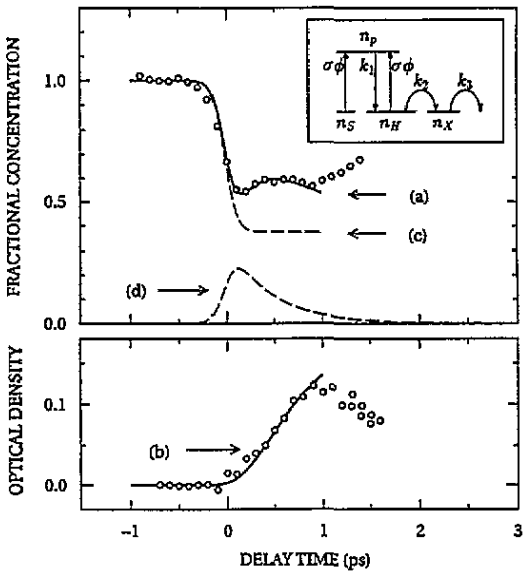

Figure 9. The calculated temporal change of the fractional concentration of the lowest triplet STEs (a) and the X centres (b), using the rate equation for the level diagram shown in the inset, including the lowest triplet STE, the 2p-excited STE, the hot STE and the X centre. The n indicate the occupation number and the other notations are those for the transition rate. The solid lines are the results of calculation and circles are experimental results. The dashed line c is the results obtained with $k_1 = 0$ and d is the rate of conversion to the hot STE.

of the X-centre concentration. The obtained best-fit parameters are

$$1/k_1 = 440 \text{ fs} \tag{5a}$$

$$1/k_2 = 430 \text{ fs} \tag{5b}$$

$$1/k_3 = 3.0 \text{ ps}. \tag{5c}$$

Figure 9 compares the calculated results with experimental results for the STE (a in the upper panel) and for the X centre (b in the lower panel); solid curves represents results of the calculation and points are experimental results. It is evident that the agreement is satisfactory.

We discuss now the relaxation route of the 2p-excited STE and the origin of the rapid partial recovery of the bleached STE band. If we put $k_1 = 0$ in (1), which means that the non-radiative recovery to the STE does not take place, $N_H(\tau_d) + N_S(\tau_d)$ is given by curve c in figure 9; it simply shows the loss of the occupation number of the STE by the photoexcitation. The difference between curves a and c is due to the rapid partial recovery of the STE (the hot STE in this approximation) from the 2p-excited STE. Thus we conclude that the STEs in vibrationally excited states are produced primarily by the de-excitation of the 2p-excited STE.

From the numerical calculation, we can evaluate the rate $C(t)(= k_1 n_p)$ of the repopulation of the STE. The curve d in the upper panel of figure 9 shows the calculated rate, not convoluted for the probe pulse shape. This repopulation rate is characterized by the time constant of 430 fs. However, its physical meaning is not straightforward, since

several steps can be involved in the transition from the optically generated 2p-excited STE to the hot STE. We discuss this point later in detail, but here we simply adopt it as a overall rate for repopulation of the STE or rate of population of the hot STE. Another point which can be made clear by this calculation is that the effect of the excitation of the hot STEs can be neglected. The calculation shows that the relative ratio of the number of the hot STEs re-excited within a light pulse to that of the hot STEs is less than 0.1. Thus, we can make essentially a single optical cycle from the lowest STE to the 2p-excited STE by our femtosecond light pulses. This makes the evaluation of the branching ratios into several pathways much easier than in experiments done by light pulses with much wider widths [28–30, 41].

4.3.2. The dynamics of the relaxation on the lowest APES. We now simulate the oscillation process in terms of the classical mechanics for particles moving on an APES with two minima. The APES was assumed to be formed by two harmonic potentials with the same characteristic frequency ω: one corresponding to the STE and the other to the X centre. The border between the STE and the X centre is defined by the crossing point Q_1 of the two harmonic potentials [45]. Therefore, it is characterized by the distance ΔQ between the two minima, and the energy difference ΔE between the two. These two quantities were treated as parameters for fitting the calculated results to the experimental results.

We can depict the dynamics of relaxation on the lowest APES in the following way. The transition from the 2p-excited state, of which the rate is given by $C(t)$, produces a local distortion which may be expressed as a wave packet on the lowest APES. In order to describe the wave packet, we introduce a Gaussian-like position function $D(Q, t')$:

$$D(Q,t') = \frac{1}{w(t')\sqrt{\pi}} \exp\left\{-\left(\frac{Q - q(t')}{w(t')}\right)^2\right\} \qquad (\text{for } t \geqslant 0) \tag{6}$$

where $q(t')$ is the coordinate of the centre of the packet at time t' after generation and $w(t')$ is a parameter which represents the width of the packet. The motion of the centre of the packet is assumed to be determined by the following classical equation of motion:

$$\frac{\mathrm{d}q}{\mathrm{d}t'} = v(t') \tag{7a}$$

$$\frac{\mathrm{d}v}{\mathrm{d}t'} = -\frac{\mathrm{d}}{\mathrm{d}q}\left(\frac{W(q)}{m}\right) - \frac{\beta}{m} v(t') \tag{7b}$$

under the initial condition

$$q(0) = Q_0 \tag{8a}$$

$$v(0) = 0. \tag{8b}$$

Here $q(t')$ and $v(t')$ are the position and the velocity at time t' after the transition to the lowest APES, and m and β stand for the mass of the particle and the coefficient of the damping term which is proportional to the velocity. The frictional force is used to introduce the energy loss during oscillation and leads finally to thermal equilibrium.

The packet may undergo a transverse relaxation that broadens the width of the packet leading to phase randomization and a longitudinal relaxation that results in dissipation of excess vibrational energy. However, knowledge of the relaxation is not available at this

moment. So, we simply assumed that the width $w(t')$ of the packet is a function of time; $w(t')$ decreases exponentially with a time constant of τ_w to converge into the width in the zeroth vibrational state of the parabola. This assumption may be too simple, but may be enough to obtain some idea of how the packet dynamics can explain the dynamical transformation between the STE and the X state.

Using the position functions, the number $n_H(t')$ of hot STEs and that $n_X(t')$ of X centres can be defined in the following way. Suppose that $n(t')$ is the total number of particles lying on the APES at time t'. Then the number $n_H(t')$ of hot STEs and that $n_X(t')$ of X centres are given by

$$n_H(t') = \int_{-\infty}^{Q_1} n(t')D(Q,t')\,dQ \tag{9a}$$

$$n_X(t') = \int_{Q_1}^{+\infty} n(t')D(Q,t')\,dQ. \tag{9b}$$

We define that the number of particles lost from the lowest APES corresponds to the number $n_F(t')$ of the F–H pairs. Because of the similar time evolution for the X centre and the F centres until 1 ps after excitation, shown in figure 6, we assume that the F–H pairs are formed only from the X centres with a rate A. Thus $n_F(t')$ and $n_X(t')$ are related by the following equation:

$$\frac{dn_X}{dt'} = -A\,n_X \tag{10a}$$

$$\frac{dn_F}{dt'} = A\,n_X - B\,n_F \tag{10b}$$

where B represents the rate of annihilation of the F–H pairs. Using the repopulation rate $C(t)$ to the lowest APES obtained previously the numbers $N_j(\tau_d)$ of the STEs, X centres and F centres are given by

$$N_j(\tau_d) = \int_{-\infty}^{\tau_d} C(t)n_j(\tau_d - t)\,dt \qquad (j = H, X, F). \tag{11}$$

These numbers were calculated numerically and fitted to the experimental results. The obtained parameters are listed in table 1.

Table 1. Parameters on the dynamics of relaxation on the lowest adiabatic potential energy surface of the excitation in NaCl.

Parameter	Value
Q_0	−4 Å
β/m	1 ps^{-1}
$\Delta E/m$	35 $Å^2\ ps^{-2}$
ω	8 ps^{-1}
τ_w	4 ps
A	0.05 ps^{-1}
B	0.5 ps^{-1}

The calculated numbers $N_S(\tau_d) + N_H(\tau_d)$, $N_X(\tau_d)$ and $N_F(\tau_d)$ for the STE, the X centre and the F centres, respectively, are shown in figure 10. In representing $N_H(\tau_d)$, we added $N_S(\tau_d)$ (figure 9 curve c) obtained from the rate equations so that the result can be directly compared with the temporal change of the STE concentration. It is evident that the simulated results are consistent with the experimental results in essential points: the presence of the oscillation, the appearance of the STE band prior to that of the X band, the gradual recovery of the STE band, the decay of the X band and the growth of the F band. The period of the oscillation, however, is reduced from 1.0 ps to 0.8 ps as τ_d increases according to the simulated results, while it is constant in the experimental results. This discrepancy arises from the improper choice of the APES, which is a combination of two one-dimensional parabolas, one having a minimum at the STE configuration and the other at the X-centre configuration. The experimental result that the period of the oscillation is almost constant for $\tau_d < 4$ ps appears to indicate that the APES for a large distortion is nearly harmonic. A small modification of the one-dimensional APES used in the present simulation or use of a multi-dimensional APES may yield better agreement. We consider that it is not worthwhile at the present stage of understanding of the atomic structures of the STE in alkali halides to elaborate this discrepancy further. Based on the results, however, we can conclude that the dynamic transformation between the STE and the X centre is due to the wave packet dynamics on the lowest APES and that the F centres are generated during the dynamic motion on the lowest APES.

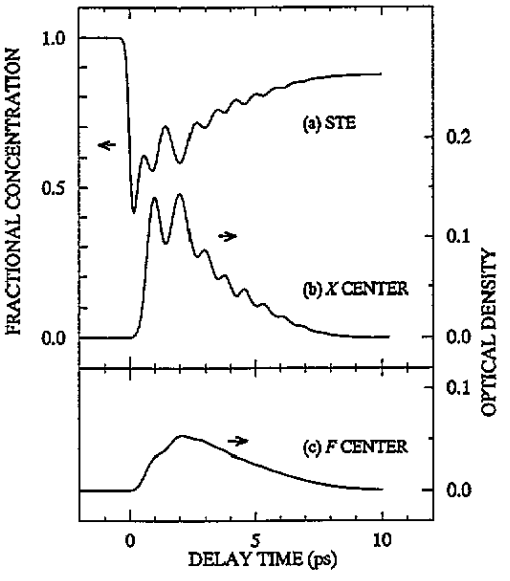

Figure 10. Simulated temporal change of the fractional concentration of the STEs and the optical density of the X band and F band after excitation of the lowest STEs to the next higher electron-excited state in NaCl.

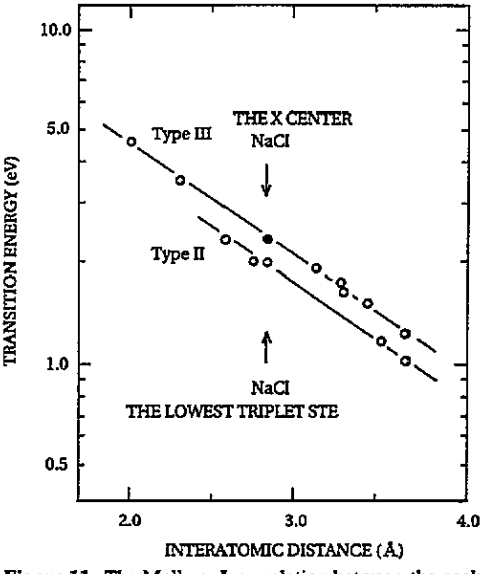

Figure 11. The Mollwo–Ivey relation between the peak energy of the electron transition band of the STE and the interionic distance in alkali halides. The upper line and lower line correspond to electron transitions due to type III STEs and type II STEs respectively. According to the relation, the X centre (solid circle) is classified into a group of type III STEs and the STE in NaCl into a group of type II STEs.

4.4. The configuration of the X centre

One of the most important findings of the present study is the experimental observation of the X centre which is a metastable excitonic state lying on the lowest APES. The band is somewhat similar to that found by Williams *et al* [36]. Here we discuss the atomic configuration of the X centre based on the experimental and theoretical results available. As described in section 1, the STEs in alkali halides have been classified into three different configurations, type I, type II, and type III. In figure 11, we reproduce the Mollwo–Ivey relation of the electron transition energy E_T of the STEs in alkali halides. E_T for the STE in NaCl is 2.0 eV at 5 K, and lies on the Mollwo–Ivey relation on the type II STE. When we plot the peak energy of the X band (solid circle in figure 11), it is seen that it lies on the line characterizing the type III STE. The result suggests that the X centre is the STE of type III in NaCl. It follows that there exist two distinctive relaxed configurations of an exciton in NaCl, although one of them, the X centre corresponding to the type III STE, is metastable.

The classification of the STE in terms of the Mollwo–Ivey relation of electron transition energy reflects only the shape of the potential for the electron of the STE. The transition energy for the STE is shallower than the corresponding transition energy of the F centre, implying that the depth of the potential is lower than that in the F centre. The shallower depth may come from the restricted relaxation of the alkali ions surrounding the vacancy due to the strong interaction with the hole component of the STE. Recent results of resonance Raman scattering spectroscopy have given microscopic information on the relaxation of alkali ions associated with the STE [25]. It has been shown that the STE in NaCl has the hole component in the form of a Cl_2^- molecular ion occupying a single halogen lattice site. Furthermore, the Raman spectra in resonance with the electron transition of the STE have shown that the distortions of the alkali ions located on the (100) plane in which the Cl_2^- molecular ion is located are significantly different from those of the F centre, while the distortions of alkali ions located perpendicular to the plane are very close to those of the F centre. The STE band due to the 1s–2p electron transition has been decomposed into three sublevels corresponding to the transitions to the symmetry-split 2p sublevels [46]. The transition energy to the level having the p-like orbital directed perpendicular to the (100) plane is higher than those having p-like orbitals directed within the plane. These results indicate clearly that the electron transition energy and hence the relaxation of alkali ions is dependent strongly on the position as well as the orientation of the Cl_2^-. Therefore, the difference in the configuration between the STE and the X centre is considered to arise from the relative position of the Cl_2^- molecular ion with respect to the vacancy where an electron is mainly localized. Here it is pointed out that the transition energy (2.13 eV) to the level with the 2p orbital oriented perpendicular to the (100) plane is very close to the peak energy of the X band, indicating that the Cl_2^- molecular ion is situated in such a way that relaxations of alkali ions are not strongly restricted in the X centre.

Puchin *et al* have studied theoretically the lowest APES of the lowest exciton in NaCl, with respect to not only the axial shift of the Cl_2^-, but also the rotational motion of the Cl_2^-, by using the *ab initio* many-electron approach and have shown that there exist several local minima on the APES [22]. Although the correspondence of these theoretically predicted minima and experimentally obtained relaxed exciton states is not straightforward at present, it is likely that the multiple minima corresponding to the STE and the X centre occur in an APES for multiple coordinates including not only the translational mode but also the rotational modes.

Here we propose that the STE (type II) in NaCl is the nearest-neighbouring pair of the F centre and the Cl_2^- molecular ion oriented along a ⟨110⟩ direction, and the X centre is of similar structure but with the axis of the Cl_2^- molecular ion rotated to some extent toward a

⟨111⟩ direction. This suggestion is supported by the theoretical results by Puchin *et al* and also by the experimental results that the Cl_2^- molecular ion in the STE in NaCl can easily rotate its axis to the other direction through a 60° jump during the relaxation [47]. The frequency of this rotational motion is not known yet, but it is considered that the frequency could be much lower than that of the stretching vibration. Thus the rotation of the Cl_2^- is a promising candidate for the reaction coordinate which connects the STE and the X centre.

4.5. Mechanism of the F–H pair formation

From the results and analysis described above, it can be safely concluded that F centres are generated in the process of dynamical relaxation on the lowest APES in NaCl. This finding gives a substantial basis to elucidate the mechanism of the F-centre formation in alkali halides, which has been studied for more than two decades. Since the first proposal by Pooley [31], the mechanism of the formation of the F centres from the STE has been discussed by several authors [6, 19, 31–35]. Although detailed reviews have been published on this topic [5], here we briefly summarize the models proposed to differentiate the concept and the processes on which each model is based. The processes of F-centre formation can be classified into two different categories: one is the thermally activated process which is dominant at higher temperatures and the other is the dynamic process which is effective in some crystals even at low temperatures. The former process is usually thought to be the thermally induced conversion of the lowest triplet STE to the F–H pair state; the decay time of the STE is correlated with the formation time of the F centre as demonstrated for KI [37] and NaCl [36]. The F-centre formation we are observing in this paper is not the thermally activated process, but is a dynamical process since experiments have been carried out at 5 K. As summarized previously [5], models for the dynamical F-centre formation are classified into two categories: one asserts that the F-centre formation is initiated at the electronically excited state of the STE [33, 34], and the other assumes that the F-centre formation occurs on the APES of the lowest STE [6, 19]. Our results indicate clearly that F centres are formed as a result of dynamic relaxation on the lowest APES, providing evidence for the latter model.

Any models which state that the F centre formation occurs on the lowest APES are based on the concept of the off-centre instability of the system comprising an X_2^- molecular ion at the D_{2h} point symmetry and a bound electron; the concept was first proposed by Toyozawa in 1978 [19]. The energy gained by this instability is imparted to the X_2^- molecular ion, which is ejected into an interstitial position to form the F–H pair. However the way the energy is dissipated during the relaxation process is considered to be strongly dependent on the structure of the potential well and the nature of the initially prepared vibrationally excited states. In this respect, we consider that the dynamical behaviour observed in the present paper may be a typical example of a system with double minima and with small efficiency of conversion into the F–H pair state. It is expected that other materials in which the structure of the lowest APES is different from that in NaCl may show different features of the dynamical process of the F-centre formation.

4.6. De-excitation pathways of the 2p-excited STE

In the analysis of experimental results, we used the function $C(t)$ as a overall rate of regenerating the STE on the lowest APES. However, the process leading to the STE on the lowest APES is presumed to involve several steps which could not be resolved in the present study: the de-excitation within 2p-excited states of the STE, non-radiative transitions from the 2p-excited STE to the lowest APES and the relaxation processes on the lowest APES until the system is relaxed to the extent that the STE band is observed. Dichroic optical

absorption measurements for the STE absorption band in NaCl have resolved three transitions to symmetry-split sublevels of the 2p-excited states of the STE [46]. Following the results of the decomposition, the photon energy of 2.05 eV (605 nm) used for the excitation is close to the peak of the transition to one of the 2p orbitals directed parallel to the (100) plane, although the bands to the other levels underlie with weaker strengths. Therefore, the photo-generated 2p-excited state of the STE may first undergo level crossing to reach the lowest levels of the 2p-excited state, and then it is transferred to the lowest APES. During this relaxation on the 2p APES, the configuration of the pair comprising an X_2^- and an electron may change from the configuration of the lowest STE. According to theoretical calculation [3, 4], the on-centre configuration in which an X_2^- molecular ion is located at the D_{2h} point group is preferred for an electron-excited state with a diffused orbital. Therefore, relaxation within the 2p-excited APES may lead to a configurational change from the off-centre to the on-centre configuration.

Soda and Itoh have studied the de-excitation process of electron-excited STEs by using the cascade-excitation technique with microsecond light pulses [41]. They have found that together with the F–H pair generation, the σ-luminescent STE is generated competitively. Since the σ luminescence is presumed to occur from the STE with the on-centre configuration, their result indicates that the on-centre STE is certainly generated in the process of the relaxation of the electron-excited STE. Therefore, it is likely that the relaxation to the lowest APES may start from the on-centre configuration.

Soda and Itoh have estimated the loss yield of the STE per optical cycle to be 0.02 when excited at 2.0 eV [41]. The evaluated value is much smaller than the result of the present direct measurement. Also, they have shown that the branching ratio between the σ-luminescent STE and the F–H pair depends strongly on the photon energy of the excitation: at 2.0 eV the ratio is 0.6, while above 2.5 eV σ luminescence is dominantly generated. Therefore, the generation of the σ-luminescent STE is an important pathway of the de-excitation of the excited states of the STE. However, the mechanism of the branching into the F–H pair and the σ-luminescent STE is not clear. Since the σ luminescence is emitted from a singlet state, intersystem crossing from the triplet manifold to the singlet one will certainly play an important role. On the other hand, the recovery of the lowest STE and the F–H pair generation through its dynamical relaxation take place on the lowest triplet APES; the spin multiplicity of the electron–hole pair is conserved. This implies that the singlet STE can maintain the on-centre configuration at least until the radiative decay of a few nanoseconds takes place, whereas the triplet STE on the on-centre configuration undergoes the off-centre relaxation within 430 fs. Thus it appears that the relaxation of the exciton depends strongly on its spin multiplicity. This is an important future problem to be solved by means of, for example, the direct excitation of electron–hole pairs by a femtosecond light pulse.

Acknowledgments

This work is supported by a grant-in-aid for specially promoted science by the Ministry of Education, Culture and Science of Japan.

References

[1] Ueta M, Kanzaki H, Kobayashi K, Toyozawa Y and Hanamura E 1986 *Excitonic Processes in Solids* (Berlin: Springer)

[2] Fowler W B and Itoh N (ed) 1990 *Atomic Processes Induced by Electronic Excitation in Nonmetallic Solids* (Singapore: World Scientific)
[3] Williams R T and Song K S 1990 *J. Phys. Chem. Solids* **51** 679
[4] Song A K S and Williams R T 1993 *Self-Trapped Excitons* (Berlin: Springer)
[5] Itoh N and Tanimura K 1990 *J. Phys. Chem. Solids* **51** 717
[6] Williams R T, Song K S, Faust W L and Leung C H 1986 *Phys. Rev.* B **33** 7232
[7] Burns A R, Stechel E B and Jennison D R (ed) 1993 *Desorption Induced by Electronic Transition* (Berlin: Springer)
[8] Brodsky (ed) 1985 *Amorphous Semiconductors* (Berlin: Springer)
[9] Koshihara S, Tokura Y, Mitani T, Saito G and Koda T 1990 *Phys. Rev.* B **42** 6853
[10] Koshihara S, Tokura Y, Takeda K and Koda T 1992 *Phys. Rev. Lett.* **68** 1148
[11] Ikezawa M and Kojima J 1969 *J. Phys. Soc. Japan* **27** 1551
[12] Kabler M N 1964 *Phys. Rev.* **136** A1296
[13] Murray R B and Keller F J 1965 *Phys. Rev.* **137** A942
[14] Murray R B and Keller F J 1965 *Phys. Rev.* **153** A993
[15] Kan'no K, Tanaka K and Hayashi T 1990 *Rev. Solid State Sci.* **4** 383
[16] Rabin H and Klick C C 1960 *Phys. Rev.* **114** 1005
[17] Tanimura K and Itoh N 1992 *Phys. Rev.* B **45** 1432
[18] Tanimura K, Itoh N, Hayashi T and Nishimra H 1992 *J. Phys. Soc. Japan* **61** 1366
[19] Toyozawa Y 1978 *J. Phys. Soc. Japan* **44** 482
[20] Leung C H and Song K S 1978 *Phys. Rev.* B **18** 922
[21] Leung C H, Brunet G and Song K S 1985 *J. Phys. C: Solid State Phys.* **18** 4459
[22] Puchin V E, Shluger A L, Tanimura K and Itoh N 1993 *Phys. Rev.* B **47** 6226
[23] Edamatsu K, Sumita M, Hirota S and Hirai M 1993 *Phys. Rev.* B **47** 6747
[24] Kayanuma Y 1990 *Rev. Solid State Sci.* **4** 403
[25] Suzuki T, Tanimura K and Itoh N 1994 *Phys. Rev.* B at press
Tanimura K, Suzuki T and Itoh N 1992 *Phys. Rev. Lett.* **68** 635
[26] Tanimura K unpublished
[27] Pooley D and Runciman W A 1970 *J. Phys. C: Solid State Phys.* **3** 1815
[28] Williams R T 1976 *Phys. Rev. Lett.* **36** 529
[29] Yoshinari T, Iwano H and Hirai M 1978 *J. Phys. Soc. Japan* **45** 936
[30] Soda K and Itoh N 1980 *J. Phys. Soc. Japan* **48** 1618
[31] Pooley D 1966 *Proc. Phys. Soc.* **87** 245
[32] Hersh H N 1966 *Phys. Rev.* **148** 928
[33] Itoh N and Saidoh M 1973 *J. Physique Coll.* **34** C9 101
Itoh N, Stoneham A M and Harker A H 1980 *J. Phys. Soc. Japan* **49** 1364
[34] Kabler M N 1975 *Proc. NATO Adv. Study Inst. on Radiation Damage Processes in Materials* ed C H S Dupuy (Leyden: Noordhoff) p 176
[35] Kabler M N and Williams R T 1978 *Phys. Rev.* B **18** 1948
[36] Williams R T, Craig B B and Faust W L 1984 *Phys. Rev. Lett.* **52** 1709
[37] Hirai M 1989 *Defect Processes Induced by Electronic Excitation in Insulators* ed N Itoh (Singapore: World Scientific) p 119
[38] Bradford J N, Williams R T and Faust W L 1975 *Phys. Rev. Lett.* **35** 300
[39] Williams R T, Bradford J N and Faust W L 1978 *Phys. Rev.* B **18** 7038
[40] Tokizaki T, Makimura T, Akiyama H, Tanimura K and Itoh N 1991 *Phys. Rev. Lett.* **67** 2701
[41] Soda K and Itoh N 1981 *J. Phys. Soc. Japan* **50** 3988
[42] Fowler W B 1968 *Physics of Color Centers* ed W B Fowler (New York: Academic) p 53
[43] As seen in figure 3(d), the optical absorption in the range of 1.8–2.0 eV is completely due to the STE. The arrival time of the 1.8 eV component of the white light at the sample position and that of the 2.0 eV component differ by about 1 ps because of the group velocity dispersion. Because of this difference, the conversion of photon energy to time delay enables us to evaluate the temporal change of the STE concentration accurately by a single shot. The analysis thus made has given exactly the same partial recovery of the bleaching of the STE.
[44] The artifact coherent term was neglected because the polarization of the probe beam was perpendicular to that of the pump beam and the temporal response was monitored at a wavelength different from that of the pump light.
[45] For the potential curve shape in the range near Q_1, we connected the two harmonic potentials continuously and smoothly by using the fourth-order polynomial $P^{(4)}(Q)$. The $P^{(4)}(Q)$ that satisfies the following conditions was used in the calculation. (1) The harmonic potentials are switched to $P^{(4)}(Q)$ continuously

and smoothly at $Q = Q_1 \pm a$. (2) $P^{(4)}(Q_1)/m = 40$ Å^2 ps^{-2}. The value of a is rather arbitrary: we found no qualitative change in the solution of (7) when a varied from 0.1 to 1.

[46] Tanimura K 1989 *Defect Processes Induced by Electonic Excitation in Insulators* ed N Itoh (Singapore: World Scientific) p 177

[47] Suzuki T, Tanimura K and Itoh N to be published